

Chemical Science

Accepted Manuscript

This article can be cited before page numbers have been issued, to do this please use: L. Naimovicius, M. Dapkevicius, E. Radiunas, M. Miroshnichenko, G. Kreiza, C. Alcaide, P. Baronas, Y. Sasaki, N. Yanai, N. Kimizuka, A. B. Pun, M. Solà, P. Bharmoria, K. Kazlauskas and K. Moth-Poulsen, *Chem. Sci.*, 2025, DOI: 10.1039/D5SC05248C.



This is an Accepted Manuscript, which has been through the Royal Society of Chemistry peer review process and has been accepted for publication.

Accepted Manuscripts are published online shortly after acceptance, before technical editing, formatting and proof reading. Using this free service, authors can make their results available to the community, in citable form, before we publish the edited article. We will replace this Accepted Manuscript with the edited and formatted Advance Article as soon as it is available.

You can find more information about Accepted Manuscripts in the [Information for Authors](#).

Please note that technical editing may introduce minor changes to the text and/or graphics, which may alter content. The journal's standard [Terms & Conditions](#) and the [Ethical guidelines](#) still apply. In no event shall the Royal Society of Chemistry be held responsible for any errors or omissions in this Accepted Manuscript or any consequences arising from the use of any information it contains.

ARTICLE

Enhancing the Statistical Probability Factor in Triplet-Triplet Annihilation Photon Upconversion via TIPS Functionalization

Received 00th January 20xx,
Accepted 00th January 20xx

DOI: 10.1039/x0xx00000x

Lukas Naimovičius,^{a,b,c} Manvydas Dapkevičius,^b Edvinas Radiunas,^b Mila Miroshnichenko,^a Gediminas Kreiza,^b Carles Alcaide,^d Paulius Baronas,^e Yoichi Sasaki,^f Nobuhiro Yanai,^f Nobuo Kimizuka,^f Andrew B. Pun,^c Miquel Solà,^d Pankaj Bharmoria,^{*a} Karolis Kazlauskas,^b and Kasper Moth-Poulsen^{*a,e,g,h}

We investigated the influence of triisopropylsilyl (TIPS) functionalization on annihilators in triplet-triplet annihilation photon upconversion, specifically focusing on their spin statistical probability factor. A new green-emitting annihilator 3,9-bis((triisopropylsilyl)ethynyl)perylene (TIPS-PY) displaying a record red-to-green TTA-UC quantum yield of 13.7% (50% theoretical maximum) is synthesized. This remarkable efficiency was achieved due to the following features of the TIPS functionalization of PY: 1) retaining a high fluorescence quantum yield of 95%, 2) reduced triplet energy to 1.29 eV enabling efficient triplet energy transfer (~100%) from the sensitizer, PdTPBP ($T_1 = 1.55$ eV), and 3) a high efficiency of singlet generation after triplet coupling, indicated by the statistical probability factor, $f = 39.2\% \pm 2.4\%$. Notably, the f value of TIPS-PY surpasses other annihilators in the 470–570 nm emission range. Excited state computational analysis using TheoDORE, revealed a higher percentage of charge transfer character in S_0S_1 in TIPS-PY compared to PY, indicative of higher singlet-like character in their triplet-pair state $^1(T_1T_1)$, which can enhance the coupling of the triplet-pair state with the excited singlet-state, thereby increasing the efficiency of singlet generation, a phenomenon undisclosed before. Furthermore, the suitable T_1 of TIPS-PY enables upconversion of 730 nm light when sensitized with Os(m-peptpy)₂(TFSI)₂ ($T_1 = 1.63$ eV), demonstrating the broad upconversion range of TIPS-PY in the phototherapeutic window desired for biological applications.

Introduction

Triplet-triplet annihilation photon upconversion (TTA-UC) is a molecular nonlinear optical process that converts two photons with low-energy into one photon with high energy (Scheme 1a).¹ This phenomenon is attractive compared to other UC processes² due to its operation under incoherent low energy density excitations³ which

opens many potential applications such as photocatalysis, biological photoactivation, 3D printing, and photovoltaics.^{4–11} A typical TTA-UC system consists of a sensitizer and an annihilator ensemble. The sensitizer absorbs low-energy photons and generates triplet states via intersystem crossing (ISC). The annihilator accumulates the triplets through Dexter triplet energy transfer (TET) from the sensitizer and undergoes TTA-UC, generating a photon-emitting high-energy singlet state (Scheme 1a). The efficiency of singlet generation is evaluated by TTA-UC quantum yield (ϕ_{UC}), which is the product of all operational processes within the TTA-UC system (eq. 1) and the spin-statistical probability factor (f). The f determines the probability of singlet generation after triplet coupling (Scheme 1b).

$$\phi_{UC} = \frac{1}{2} f \phi_{ISC} \phi_{TET} \phi_{TTA} \phi_{FL} \quad (1)$$

In the eq. 1, ϕ_{UC} , ϕ_{ISC} , ϕ_{TET} , ϕ_{TTA} , ϕ_{FL} represent the quantum yields of upconversion (UC), intersystem crossing (ISC), triplet energy transfer (TET), triplet-triplet annihilation (TTA), and annihilator fluorescence (FL), respectively.

The f plays an essential role in TTA-UC by defining the maximum achievable ϕ_{UC}^0 as $f/2$ when all other processes approach unity. As follows, the f allows us to assess the intrinsic potential of the annihilator triplets to generate an emissive singlet state (Scheme 1b). It can be altered by suitable molecular engineering of annihilator

^a Institute of Materials Science of Barcelona (ICMAB-CSIC) Universitat Autònoma de Barcelona Bellaterra, Barcelona, 08193, Spain.

^b Institute of Photonics and Nanotechnology Vilnius University Saulėtekio av. 3, LT-10257 Vilnius, Lithuania

^c Department of Chemistry and Biochemistry University of California San Diego 92093 La Jolla, CA, USA

^d Institute of Computational Chemistry and Catalysis (IQCC) Universitat de Girona M. Aurèlia Capmany 69, 17003 Girona, Spain

^e Department of Chemical Engineering Universitat Politècnica de Catalunya EEBE Eduard Maristany 10–14, 08019 Barcelona, Spain

^f Department of Applied Chemistry, Graduate School of Engineering Kyushu University 744 Moto-oka, Nishi-ku, Fukuoka 819-0395, Japan.

^g Catalan Institution for Research & Advanced Studies (ICREA) Pg. Lluís Companys 23, Barcelona, Spain

^h Department of Chemistry and Chemical Engineering Chalmers University of Technology Kemivägen 4, Gothenburg 412 96, Sweden

† Supplementary Information I and II are available: [details of any supplementary information available should be included here]. See DOI: 10.1039/x0xx00000x

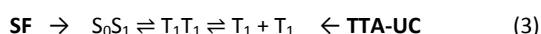
*E-mails – kasper.moth-poulsen@upc.edu; pbharmoria@icmab.es



chromophores to control the triplet coupling strength, which has been investigated in this work. The TTA results in the formation of a triplet-pair ($T_1 \cdots T_1$) whose net spin can be $S = 0, 1$ or 2 , hence possessing singlet, triplet, or quintet character. According to the adapted Merrifield model including exchange interactions (J), under zero-field splitting, coupling results in the formation of 9 spin eigenstates of $T_1 T_1$ pairs with an overall fraction of $1/9, 3/9$ and $5/9$ of singlet, triplet, and quintet pair states (Scheme 1b). Triplet coupling can be simply expressed by Heisenberg's spin-only Hamiltonian (\hat{H}) using eq. 2

$$\hat{H} = -2J\hat{S}_1 \cdot \hat{S}_2 \quad (2)$$

where \hat{S}_1 and \hat{S}_2 are individual spin operators of the two individual interacting triplets, and J is the magnetic exchange parameter that also defines the strength of inter-triplet exchange interactions.^{1,5} In the case of strong electronic coupling, the quintet state (Q_1) is energetically inaccessible and cannot form the excited singlet state. This limits the f of singlet formation to $1/4$, leading to low UC efficiencies. However, the quintet and triplet (T_2) states may re-participate in singlet formation via other channels like Q_1 to T_1 dissociation, and T_2 to T_1 internal conversion (IC).^{12,13} This recycling can increase the experimentally obtained f value even up to $\sim 1/2$.^{5,14,15} The TTA-UC ($^1(T_1 T_1) > S_1 S_0$) is the reverse process of singlet fission ($S_1 S_0 > ^1(T_1 T_1)$) with an intermediate correlated triplet pair state, $^1(T_1 T_1)$ as per the Johnson–Merrifield model eq. 3.^{16,17}



It is according to the Merrifield model that the singlet character of the $T_1 T_1$ pair determines its coupling to the singlet state.¹⁸ Hence, annihilators with a triplet-pair state exhibiting a significant singlet character can have a high probability of singlet formation and consequently, a higher f factor¹⁹ which has been investigated in this

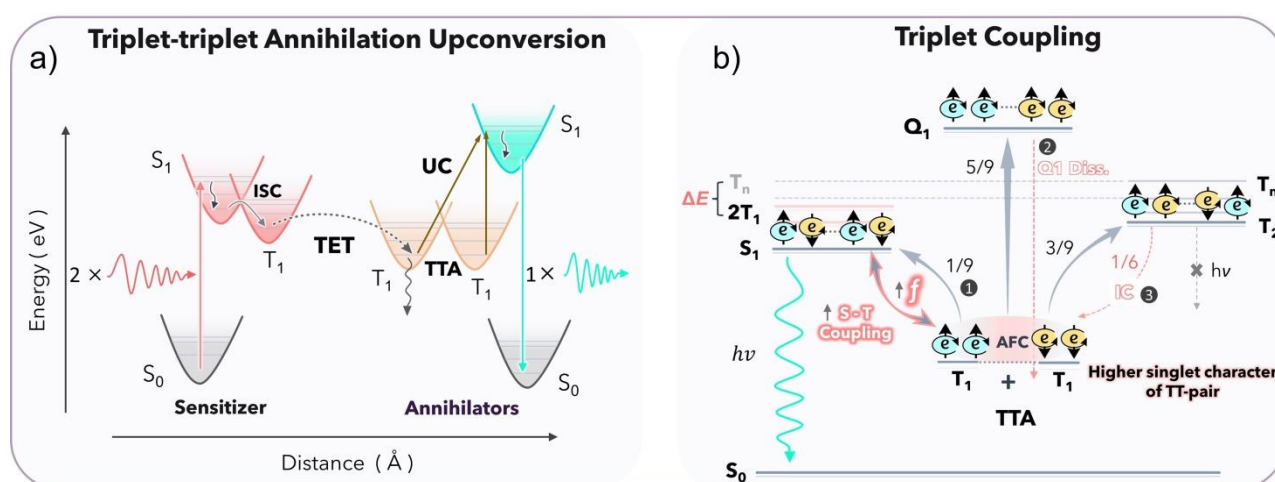
work by calculating the percentage of charge resonance/transfer character in the $S_0 S_1$ dimer.
DOI: 10.1039/D5SC05248C

Another way to increase the f factor is to avoid secondary loss channels such as $2T_1$ to T_n non-radiative decay (Scheme 1b). This can be achieved via the molecular engineering of an annihilator with $2T_1 \approx S_1$ and Q_n and T_n states higher in energy than the $2T_1$ state. This prevents $2T_1$ decay to Q_n or T_n states due to the energy gap law relation⁵ (eq. 3). This results in preferential decay of $2T_1$ to the S_1 state, leading to more efficient singlet generation.

$$k_{nr} \sim \exp\left(\frac{-\gamma|\Delta E|}{\hbar\omega_M}\right) \quad (4)$$

where k_{nr} is the rate of non-radiative decay and ΔE is the energy gap between electronic states.

Several derivatives of naphthalene,^{14,20} anthracene,^{21–23} perylene,^{24,25} rubrene,^{26–30} and diketopyrrolopyrrole^{31,32} based compounds have been investigated to achieve high f values to boost the overall ϕ_{UC} .⁵ The UC emission of these compounds spans across the majority of the UV-visible spectrum. However, the lack of an efficient annihilator emitting within the 470–540 nm range impedes important biological applications which can be photoactivated with upconverted green light upon excitation within or close to the phototherapeutic window (650–850 nm).³³ These applications include targeted drug delivery,³⁴ light-gated ion channel control,³⁵ light-activated CRISPR,³⁶ photo-pharmacology,³⁷ and photosynthesis.³⁸ While 9,10-Bis(phenylethynyl)anthracene (BPEA) is a well-known commercially available green annihilator, its low UC quantum yield due to the small $f = 5.6$ to 6.3% is an issue.²¹ Therefore, an efficient annihilator within the 470–540 emission range may become a powerful photoactivation tool in biological applications upon low-density red or NIR excitation via TTA-UC for embracing higher penetration into biological tissue.



Scheme 1. a) Scheme of TTA-UC indicating conversion of two low-energy photons into one high-energy photon through a series of energy transfer processes. ISC - intersystem crossing, TET - triplet energy transfer, TTA – triplet-triplet annihilation and UC - upconversion b) Schematic illustration of the post-TTA events resulting in the formation of the TT pair with singlet (S_1 , $f = 1/9$), triplet (T_2 , $3/9$) and quintet (Q_1 , $5/9$) states due to the anti-ferromagnetic coupling (AFC) between triplet-pairs. Further recycling via quintet dissociation (Q_1 diss.) or internal conversion (IC) can increase the f of S_1 formation to $1/2$. A higher singlet character of the TT pair increases the coupling between the TT pair and the singlet state, which further increases the f .

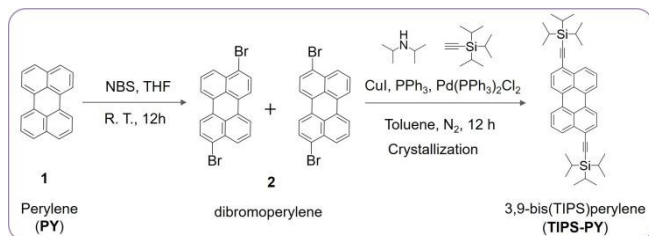


Herein, we report the synthesis of a new perylene (PY) based annihilator functionalized with triisopropylsilyl (TIPS) groups, **TIPS-PY** (Fig. 1a). **TIPS-PY** demonstrates highly efficient TTA-UC, with experimental ϕ_{UC} of 13.7% (out of 50%), with $f = 39.2\%$ upon combining with Pd(II) meso-tetraphenyl tetrabenzoporphine (PdTPBP) as sensitizer ($\lambda_{ex} = 640$ nm CW laser). The ϕ_{UC} is shown to be greater compared to unfunctionalized **PY** due to the increase in f value implying enhanced triplet-pair-singlet coupling, which may be governed by the singlet-like character of the triplet-pair state of **TIPS-PY**, revealed from the higher percentage charge resonance or charge transfer character of the S_0S_1 excitations of the **TIPS-PY** compared to **PY** using TheoDOR program.^{19,39} To our knowledge, an efficient annihilator in 470–540 nm emission range with a high f value of $39.2\% \pm 2.4\%$ and ϕ_{UC}^∞ up to 19.6% (theoretical limit) has not been reported before.⁴⁰ This study demonstrates the value of TIPS-functionalization in engineering the triplet energy, singlet-triplet character, and T_1T_1 coupling of annihilator triplets to yield a high statistical probability factor for upconverted singlet-state generation, which is a key limiting factor in TTA-UC. When combined with Os(m-peptpy)₂(TFSI)₂ as a sensitizer, **TIPS-PY** upconverted the 730 nm light into yellow-green light, thus reaching deep into the phototherapeutic window³³ that is highly sought after for various biological applications^{34–38}

Results and discussion

Synthesis of 3,9-bis((triisopropylsilyl)ethynyl)perylene (TIPS-PY)

The annihilator, **TIPS-PY** was synthesized in a two-step reaction as depicted in Scheme 2. A mixture of 3,9- and 3,10-dibromoperylene was obtained via an electrophilic aromatic bromination reaction between **PY**, and *n*-bromosuccinimide (NBS).⁴¹ The final compound, **TIPS-PY**, was obtained via a Sonogashira coupling between the mixture of 3,9- and 3,10-dibromoperylene and TIPS-acetylene. The purified orange colored compound was characterized by ¹H NMR, ¹³C {¹H} NMR, MALDI-TOF, and single-crystal X-ray diffraction analysis (for detailed synthesis procedure and characterization see Annexure 1, Fig. S1–S5) and found to be 3,9-bis(TIPS)perylene.



Scheme 2. Synthesis of 3,9-bis(TIPS)perylene (**TIPS-PY**)

Photophysical Properties

The photophysical properties of **TIPS-PY** were studied in comparison to other competitive annihilators, **PY** and **BPEA** in the 470 to 540 nm emission range. The molecular structures of **TIPS-PY**, **PY**,⁴² and **BPEA**²¹ are shown in Fig. 1a along with PdTPBP, the sensitizer used in this study for red-to-green upconversion.

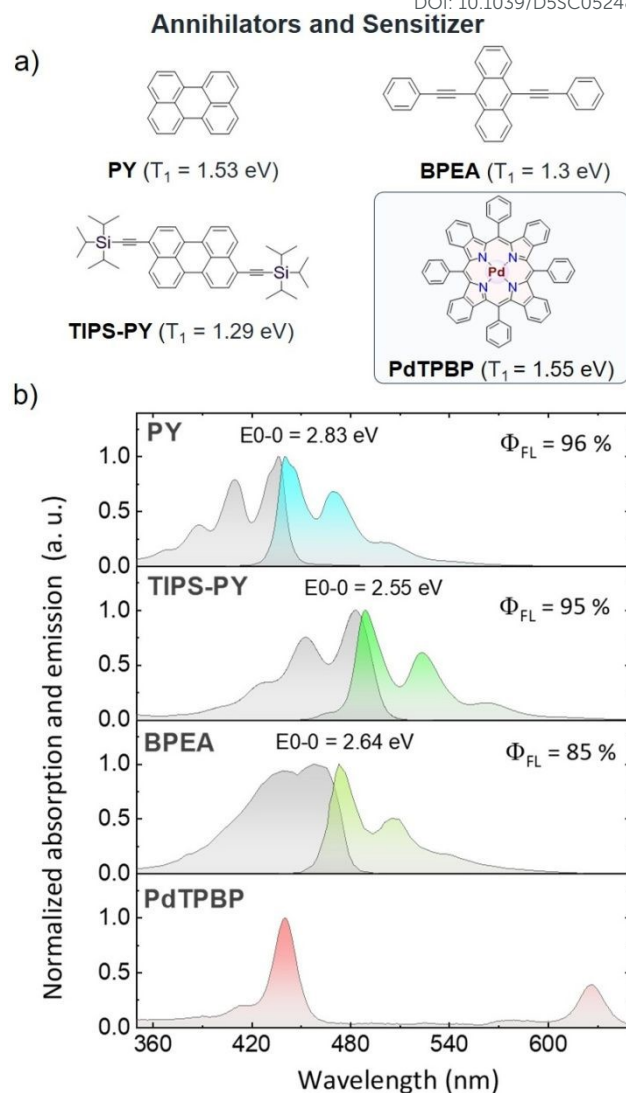


Fig. 1. Molecular structures and T_1 energies (a), and absorption and emission spectra (b) of annihilators (**PY**, **TIPS-PY**, **BPEA**), and sensitizer (**PdTPBP**) at concentrations of 20 μ M and 1 μ M in THF, respectively.

TIPS-PY demonstrated absorption and emission peaks at 483 nm ($\epsilon \sim 73000$ M⁻¹ cm⁻¹, Fig. S6) and 489 nm ($\phi_{FL} = 95\%$ and $\tau_{FL} = 5.5$ ns), respectively (Fig. 1b, S7, and S8). Compared to **PY**, the emission spectrum of **TIPS-PY** is red-shifted by 0.29 eV due to the extension of conjugation upon introduction of TIPS-acetylene moieties (Fig. 1b). However, the ϕ_{FL} remained almost the same (96% and 95%). This red shift in the emission spectrum of **TIPS-PY** overcame the secondary inner filter issue caused by reabsorption of UC light by the **PdTPBP** Soret band to boost the ϕ_{UC} (Fig. S9). When compared to **BPEA**, the emission spectrum of **TIPS-PY** is red-shifted by just 0.1 eV (Fig. 1b). However, the lower $\phi_{FL} = 85\%$ ²¹ of **BPEA** implies a negative effect on the overall ϕ_{UC} according to Eq. 1. Besides ϕ_{FL} , our previous time dependent density functional theory (TD-DFT) investigations (Gray et al.²¹) found that the difference in geometry of singlet and triplet surfaces of **BPEA** makes the triplet-state energetically inefficient to generate the first excited singlet-state to yield low ϕ_{UC} .²¹ Hence, prior to TTA-UC experiments, molecular geometry optimization, and excited state modeling studies of **TIPS-PY** in comparison to **PY** were conducted (Fig. 1 and Fig. S10).



Excited-State Modeling Studies

The DFT and TD-DFT calculations carried out at the (U)PBE0-D3(BJ)/6-311G(d,p) level of theory have shown the T_1 states of **PY** and **TIPS-PY** at 1.49 eV and 1.29 eV, respectively (see SI for a more detailed description of the computational method). The calculated T_1 of **PY** is almost similar to the reported experimental,⁸ and theoretical values ~ 1.5 eV.⁴² The calculated singlet-state (S_1) energies of **PY** and **TIPS-PY** (Fig. S10) are also in agreement with the experimental S_1 values. Due to the T_1 of **TIPS-PY** at 1.29 eV, **PdTPBP** having T_1 at 1.55 eV⁴² (Fig. 1a) was selected as a sensitizer to ensure the feasible sensitization of **TIPS-PY** via an exothermic triplet energy transfer pathway. Moreover, the non-overlapping of the emission spectrum of **TIPS-PY** with the absorption spectrum of **PdTPBP** (Fig. 1b and S9), and a high ϕ_{ISC} of **PdTPBP** approaching unity⁴⁴ were other key factors for **PdTPBP** selection as a sensitizer.

The calculated energy level distributions (Fig. S10) demonstrate that **TIPS-PY** complies with the $2T_1 > S_1$ energetic condition for TTA-UC to occur.⁵ However, the proximity of $2T_1$ to higher energy triplet-states ($T_n = T_2, T_3$) plays a crucial role in the probability of singlet generation due to the energy gap law relation (equation 4), imposing a non-radiative decay channel if $2T_1$ is in the vicinity of T_2 and further from S_1 .⁴⁵⁻⁴⁶ We investigated the implication of the energy gap law in affecting the f factor of **TIPS-PY** and found a $2E_{T_1}-E_{T_2}$ energy gap of +70 meV. The gap is significant enough to substantially reduce the non-radiative decay.⁴⁵⁻⁴⁷ Hence it could be one of the key contributors to the high f factor of **TIPS-PY**. However, when compared with the $2E_{T_1}-E_{T_2} = -140$ meV of **PY** having f value of 17.9%⁴² this parameter does not seem enough to explain the high f factor observed of **TIPS-PY**. Hence, we explored another possible channel to understand the high f factor of **TIPS-PY**. One key argument of the Merrifield model of triplet-triplet coupling is that the efficiency of singlet generation depends on the triplet pair-singlet coupling.^{18,29,48} Hence, a higher singlet character of the triplet-state can increase the singlet-triplet coupling post triplet-triplet annihilation to generate a high singlet population.¹⁸ Therefore, we calculated the charge resonance or charge transfer character of S_1S_0 , commonly shared by $^1(T_1T_1)$, of **TIPS-PY** compared to that of **PY** to assess the singlet character using TheoDore program (Fig.).^[39] Fig. 2a, shows the change in electron density from the ground state to the excited state, resulting from a linear combination of orbital replacement involving charge transfer (blue arrows) and local excitations (black arrows). The HOMO-1 to LUMO+1 transition in **TIPS-PY**, which contributes the strongest (92.39%), has charge transfer (CT) character, moving one electron each from left to right and from right to left. Contrary to this, the HOMO-1 to LUMO+1 transition in **PY**, which contributes the strongest (88.24 %), has a charge resonance (CR) character. The percentage of CT or CR character is indicative of the singlet character of the dimer.³⁹ These results indicate that TIPS-functionalization increases the singlet character of the **TIPS-PY** dimer, which is likely to have a positive effect on f value (Scheme 1b)^{16,49-51} and UC quantum yield.

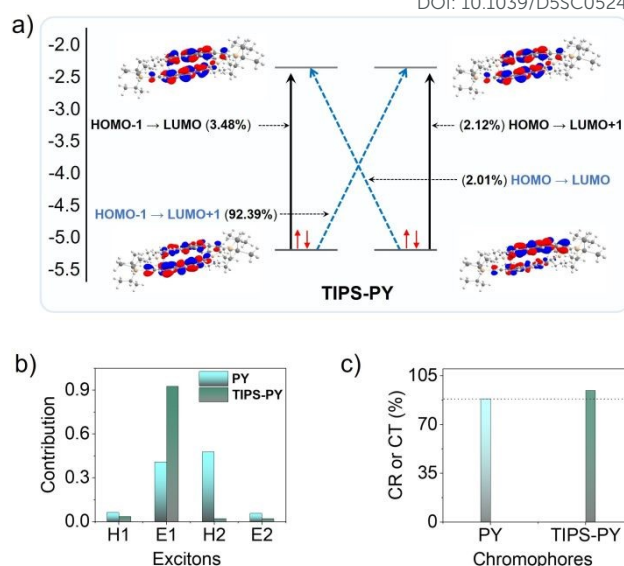


Fig. 2. a) Illustration of the contribution of the linear combination of orbital replacement in **TIPS-PY**. b) Plot showing comparative electron (E), and hole (H) contributions during orbital replacement in **PY** and **TIPS-PY**. c) Percentage of charge resonance (CR) or charge transfer (CT) calculated from E and H contributions during orbital replacement in **PY** and **TIPS-PY**.

To substantiate these results, we also investigated biphenyl (**BP**) and bis-TIPS-biphenyl (**TIPS-BP**), having a similar transition dipole axis as that of **PY** (Fig. S11a, b)⁵²⁻⁵³ using the TheoDore program (Fig. S12). Similar to **PY**, the CT character of **BP** increased upon TIPS-functionalization (Fig. S12d), thus supporting the proposed argument. Recently, **TIPS-BP** was shown to demonstrate superior UC performance compared to **BP**, confirming our prediction experimentally.⁵⁴ Seeking further generalization of this argument, we also calculated the CT or CR character for highly efficient TIPS-functionalized annihilators such as TIPS-anthracene (**TIPS-An**)²³ and TIPS-naphthalene (**TIPS-Naph**).⁵⁵ However, the CT or CR character decreased for these molecules upon TIPS-functionalization (Fig. S13a-d). This could be due to the difference in the main transition dipole axis of **Naph** and **An** (1L_a), which unlike **BP** and **PY** is along the horizontal axis (Fig. S11b). It is to mention that the transition dipole axis plays a key role in the electronic interactions of the molecules in the excited state.⁵⁶ Nevertheless, it shows that the singlet character of the triplet pair may not be the sole criterion to evaluate the high TTA-UC quantum yields in molecules with different transition dipole axes. Therefore, we also investigated the role of energy gap law⁵ in **TIPS-An** and **TIPS-Naph** and found $2E_{T_1}-E_{T_2}$ of -103 meV, and +186 meV, respectively (Table S2), which is in synergy with results obtained upon application of the energy gap law in the case of **PY** and **TIPS-PY**. Therefore, the energy gap law could be the common factor contributing to high ϕ_{UC} (27%)²³ of **TIPS-An** and high f value (54%)⁵⁵ of **TIPS-Naph** chromophores, as well as **TIPS-PY**. Seeking further insights, we also computed the S_0S_0 and T_1T_1 states for **PY** and **TIPS-PY** and found a smaller dimerization energy for **TIPS-PY** (-31.6 kcal/mol) compared to that of **PY** (-20.43 kcal/mol) (see Fig. S14).⁵⁷ In both cases, the potential energy surface is relatively flat, allowing for easy rotation and translation of the dimers. In the particular case of **PY**, we have also computed the S_0S_1 , S_0T_1 , S_0T_2 , and T_1T_2 states (Fig. S15). As the emission of



TIPS-PY is red-shifted due to the presence of **TIPS** moieties, the extended conjugation leads to a decrease of excited state energies (Fig. 1a) as well as the polarization of the $C \equiv C$ bond in the opposite direction by the triplet spin compared to **PY** (Fig. S16). The higher stability of the T_1 state in **TIPS-PY** can be attributed to the reduction of the HOMO-LUMO gap by 0.37 eV in **TIPS-PY** compared to **PY**.⁵⁷ Given the extension of conjugation, the T_1 energy of **TIPS-PY** (1.29 eV) decreased by 0.24 eV compared to **PY** (1.53 eV) making it suitable for exothermic triplet-energy transfer.

Triplet-Triplet Annihilation Photon Upconversion

Following photophysical characterization and excited-state modeling studies, the **TIPS-PY** annihilator was applied in TTA-UC in combination with **PdTPBP** as a sensitizer in deaerated THF. The investigated **TIPS-PY**:**PdTPBP** UC system demonstrated UC emission upon 640 nm laser excitation (Fig. 3a,b and Fig. S17), confirming the DFT prediction of the most favourable energetic condition ($2T_1 \geq S_1$) for TTA-UC.⁵ To demonstrate the full potential of **TIPS-PY**, the annihilator concentration was varied from 0.1 mM to 100 mM while the **PdTPBP** concentration was maintained at 0.01 mM (Fig. 3a-b). The **TIPS-PY**:**PdTPBP** system demonstrated a high experimental ϕ_{UC} varying from 7.0% to 13.7% (Fig. 3b and Table 1) at 100 mM and 1 mM annihilator concentrations, respectively. The ϕ_{UC}^∞ and UC threshold (I_{th}) were estimated from ϕ_{UC} vs. excitation power density (I_{ex}) profile according to previously reported procedures⁵⁸ (Fig. S18 and Table 1).

The I_{th} values for **TIPS-PY**:**PdTPBP** varies from 0.19 W cm⁻² to 0.43 W cm⁻², a low threshold barrier desired for most applications. The difference in ϕ_{UC}^∞ at varying **TIPS-PY** concentrations can be explained by concentration effects on ϕ_{FL} and ϕ_{TET} according to eq. 1. While the ϕ_{FL} (75.5% - 73.5%) for 0.1 mM to 10 mM concentrations are similar, the 100 mM concentration sample demonstrates a decrease in ϕ_{FL} to 65.5% owing to the aggregation of the annihilator species (Fig. 3a and Fig. S19). This suggests an enhanced non-radiative decay channel, potentially due to the aggregation. It was also reflected in the anti-Stokes shifts, which varied from 0.56 to 0.21 eV between 0.1 to 100 mM **TIPS-PY** (Table S3).⁵⁹ No significant aggregation is observed up to a concentration of 10 mM, as evidenced by the absence of changes in the low-energy shoulder of the absorption spectra (Fig. S20). The growth of

ϕ_{TET} from 96% to 100% is explained by the higher concentration of acceptor chromophores surrounding sensitizer molecules. The longest triplet-lifetime, $\tau_T = 1250 \mu s$ was observed at the lowest **TIPS-PY** concentration (0.1 mM), and decreased further upon increasing the concentration (Table 1 and Fig. S21).

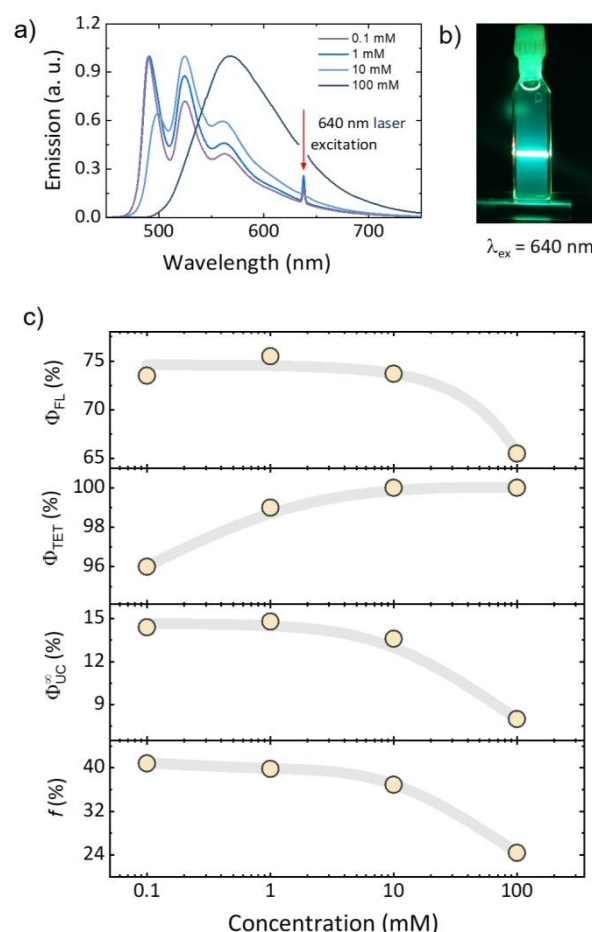


Fig. 3. a) **TIPS-PY**:**PdTPBP** upconversion spectra at 0.1 mM, 1 mM, 10 mM, and 100 mM annihilator concentrations. 640 nm laser excitation indicated. b) Digital image of TTA-UC emission, and c) ϕ_{FL} , ϕ_{TET} , ϕ_{UC}^∞ and f dependence on **TIPS-PY** concentration. All solutions were prepared in deaerated THF. **PdTPBP** concentration in all UC solutions was maintained at 0.01 mM. The grey lines serve as guide to the eyes.

Table 1. UC parameters of **TIPS-PY**:**PdTPBP** UC solutions in deaerated THF at 0.1 mM, 1 mM, 10 mM, 100 mM, and 0.01 mM concentrations of **TIPS-PY** and **PdTPBP**.

TIPS-PY	$\phi_{FL}^{[a]}$, %	$\phi_{UC}^{[b]}$, %	$\phi_{UC}^\infty^{[c]}$, %	$\phi_{TET}^{[d]}$, %	$I_{th}^{[e]}$, W cm ⁻²	$\tau_T^{[f]}$, μs	$f^{[g]}$, %
0.1 mM	73.5	11.1	14.4	96	0.19	1250	40.8
1 mM	75.5	13.7	14.9	99	0.29	914	39.8
10 mM	73.7	13.0	13.6	100	0.43	741	36.9
100 mM	65.5	7.0	8.0	100	4.94	30-80	24.4

^[a] FL quantum yield of annihilator in UC solution. ^[b] reabsorption corrected maximum measured UC quantum yield values ^[c] maximum attainable UC quantum yield values. ^[d] TET quantum yield. ^[e] UC threshold at 38.2% of ϕ_{UC}^∞ . ^[f] triplet lifetime ($= 2 \times \tau_{UC}$). ^[g] statistical probability of singlet generation from two triplets via TTA, calculated according to eq. 1. τ_{UC} values in Table 1 were determined from the tail fit of the UC emission decay profiles in Fig. S21.



ARTICLE

This decreases the average distance between **PdTPBP** and **TIPS-PY**, inferring higher TET probability. ϕ_{TET} was evaluated *via* rise time (τ_r) of TTA-UC transients (Fig. S22 and Table S4) according to the following relation:

$$\phi_{TET} = 1 - \frac{2\tau_r}{\tau_0} \quad (5)$$

where τ_0 – intrinsic (unquenched) triplet lifetime of the sensitizer that, in the case of **PdTPBP**, is 175.5 μ s.⁴² A high ϕ_{TET} = 96 % was also confirmed from the quenching of the phosphorescence spectrum of **PdTPBP** by **TIPS-PY** (Fig. S22).

To further understand the higher TTA-UC quantum yields obtained with **TIPS-PY**, the f value of $39.2\% \pm 2.4\%$ was evaluated according to eq. 1 as the average of 3 measurements at 0.1 mM, 1 mM, and 10 mM annihilator concentrations (Fig. 3b and Table 1). The results obtained at 0.1 mM, 1 mM, and 10 mM support that f value is an intrinsic property of a molecule that does not experience a change due to the change in concentration. The f value of 24.4% recorded at 100 mM was omitted from the calculation due to the presence of **TIPS-PY** aggregates (Fig. 3a and Fig. S19) in the UC solution enabling non-radiative decay channels.

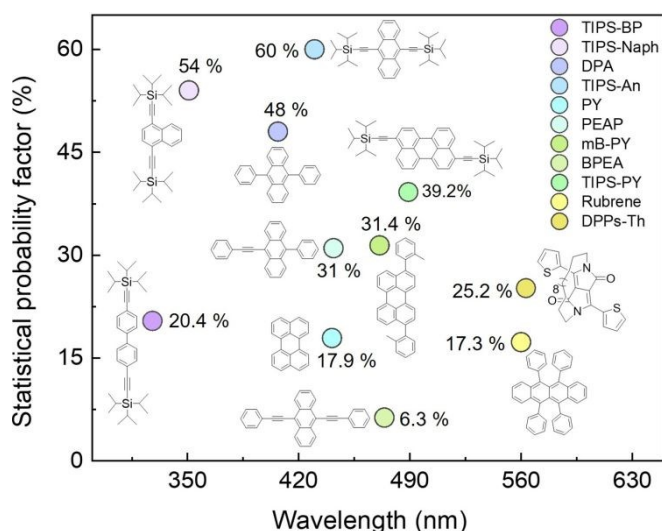


Fig. 4. Plot showing variation in statistical probability factor of various annihilators emitting across the visible spectral range. **TIPS-PY** synthesized in this work tops the list in the 470-570 nm range.

For a reliable comparison of f values between studied **PY**,⁴² **TIPS-PY**, and **BPEA**, we conducted additional measurements at identical conditions with **BPEA:PdTPBP** UC system to determine the f value resulting in 6.3% (Fig. S23, S24, and Table S6). The reported f value of $39.2\% \pm 2.4\%$ for **TIPS-PY** outperforms all previously studied

annihilators within the 470-570 nm emission region and is among the top values in the entire spectrum (Fig. 4).^{5, 40, 54, 60-62} This leads to a high experimental ϕ_{UC} of 13.7% with a possibility to extend the value until the intrinsic limit $\phi_{UC}^{\infty} \sim 19.6\%$ if all energy transfer processes approach unity. The main reason for the high f value of **TIPS-PY** is the TIPS functional groups, which increase the stability of the triplet state as well as form a singlet-like character of the triplet dimer (T_1T_1) species, as revealed from the charge resonance or charge transfer studies. This may exhibit a positive impact on $T_1 \cdots T_1$ pair state and S_1 coupling to generate the singlet-state with high efficiency according to the Merrifield model.^{18,29,48} Additionally, the favourable energy distribution prevents $2T_1$ -to- T_2 non-radiative decay from favouring the S_1 formation.

We also investigated the rate of TTA (k_{TTA}) as a possible reason for higher UC performance in **TIPS-PY** compared to **PY** in THF. To determine k_{TTA} of **TIPS-PY**, UC intensity decay profiles of **TIPS-PY:PdTPBP** and **PY:PdTPBP** solutions containing 0.1 mM of annihilator were measured at increasing excitation power densities (Fig. 5) and fitted using the following relation.⁶³

$$I(t) \propto [{}^3A^*(t)]^2 = \left([{}^3A^*]_0 \frac{1-\beta}{\exp(t/\tau_T) - \beta} \right)^2 \quad (6)$$

$$\beta = \frac{2k_{TTA}[{}^3A^*]_0}{2k_{TTA}[{}^3A^*]_0 + k_T} \quad (7)$$

Here, $[{}^3A^*]_0$ denotes the initial triplet exciton concentration within the annihilator, and τ_T ($= 1/k_T$) is the spontaneous triplet decay lifetime. τ_T was obtained from the tails of the transients, assuming that the condition $k_T \gg k_{TTA}[{}^3A^*]_0$ is met at low triplet exciton concentration, where TTA is negligible.

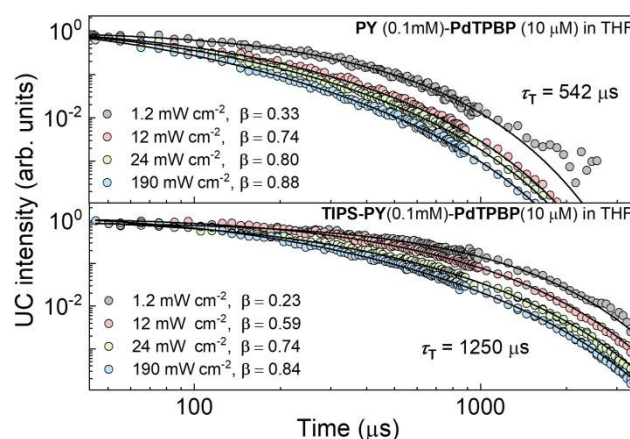


Fig. 5. Normalized UC transients of **PY** and **TIPS-PY** on a log-log scale at different excitation densities (indicated) upon sensitization with **PdTPBP** at 640 nm. Circles present experimental data, while solid lines show global fits with a shared τ_T .



The obtained β values, which describe TTA efficiency at particular excitation densities, are listed in Table S5, along with τ_T values. Since pulsed nanosecond excitation with a pulse duration much shorter than triplet lifetime was used, quasi-steady-state conditions could not be achieved, preventing direct determination of $[^3A^*]_0$ from these measurements. However, given that the τ_T is known and remains invariant with excitation density, $[^3A^*]_0$ at each pump level was estimated utilizing the reported k_{TTA} value for **PY** ($19 \times 10^8 \text{ M}^{-1} \text{ s}^{-1}$)⁶⁴ according to the eq. 7. Considering the similar TET efficiencies for **PY:PdTPBP** ($\phi_{TET} = 92\%$)⁴² and **TIPS-PY:PdTPBP** ($\phi_{TET} = 96\%$; this work) at equivalent annihilator and sensitizer concentrations, the $[^3A^*]_0$ values derived for **PY:PdTPBP** were also employed to estimate k_{TTA} in **TIPS-PY**. The estimated k_{TTA} for **TIPS-PY** is approximately $5 \times 10^8 \text{ M}^{-1} \text{ s}^{-1}$, which is 4-fold lower than that of **PY**. Hence, k_{TTA} may not be the reason for higher UC performance in **TIPS-PY** compared to **PY**. This observation is different from what has been reported by Han et al.⁴⁰ where the higher normalized triplet-triplet annihilation efficiency of 3,10-di-*o*-tolylperylene (**mB-PY**) triplets, due to the restricted motion of *o*-tolyl rings was cited as the key reason for enhanced UC quantum yield.⁴⁰ Nevertheless, the enhancement of UC performance by **TIPS** groups provides a novel strategy for molecular design for future annihilators as well as demonstrates the potential of **TIPS-PY** as another suitable compound to be implemented in numerous applications, especially in biology requiring 470-540 nm emission upon excitation with deep tissue penetrative red/far-red light.

To further demonstrate the potential of the **TIPS-PY** for long-wavelength far-red light upconversion, we performed TTA-UC study by combining **TIPS-PY** with **Os(m-peptpy)₂(TFSI)₂** as sensitizer in deaerated DMF (Fig. 6a). The absorption spectrum of **Os(m-peptpy)₂(TFSI)₂** shows vibronic peaks at 291, 318, 422, 447 nm due to ligand centred, at 494 nm due to singlet metal-to-ligand charge transfer (¹MLCT) and at 648 nm and 673 nm due to triplet MLCT (³MLCT) respectively (Fig. 6b).⁶⁵ Furthermore, **Os(m-peptpy)₂(TFSI)₂** shows ³MLCT emission at 759 nm (1.63 eV) and phosphorescence emission due to meta-substituted perylene units at 827 nm (1.5 eV), respectively.⁶⁵ Unlike other Os-complexes, it shows a long phosphorescence lifetime (τ_{PO}) of 98 μs (Fig. S25), which is among the key requirements for an efficient sensitizer in TTA-UC.⁵ Upon excitation with 730 nm CW laser, the **TIPS-PY:Os(m-peptpy)₂(TFSI)₂** (1mM:0.01mM) system demonstrated bright yellow-green UC emission (Fig. 6c,d), thus expanding the upconversion range into the phototherapeutic window to the far-red region.³³ The phosphorescence transients (Fig. S25) were used to determine the $\phi_{TET} = 99.7\%$, indicating almost complete quenching of **TIPS-PY:Os(m-peptpy)₂(TFSI)₂** phosphorescence by **TIPS-PY**. Despite the high ϕ_{TET} , long triplet lifetime, $\tau_T = 846 \mu\text{s}$ (Fig. S26) and high $\phi_{FL} = 71\%$ of **TIPS-PY** in this system, a low absolute $\phi_{UC} = 0.62\%$ was observed. This could be due to 1) the secondary inner filter effect caused by fast reabsorption of the upconverted light by **Os(m-peptpy)₂(TFSI)₂** due to the high spectral overlap of its absorption spectrum with the emission spectrum of **TIPS-PY** (Fig. 6b and Fig. S27), or 2) aggregated UC emission due to complexation of **TIPS-PY** with **Os(m-peptpy)₂(TFSI)₂** confirmed from the distorted UC

emission spectrum showing shift in emission maxima to 572 nm in the yellow emission range (Fig. 6c). Comparatively low solubility of **TIPS-PY** in DMF also support the possible aggregated UC emission. A better far-red absorbing sensitizer with higher transparency window in the **TIPS-PY** emission range may yield higher ϕ_{UC} .

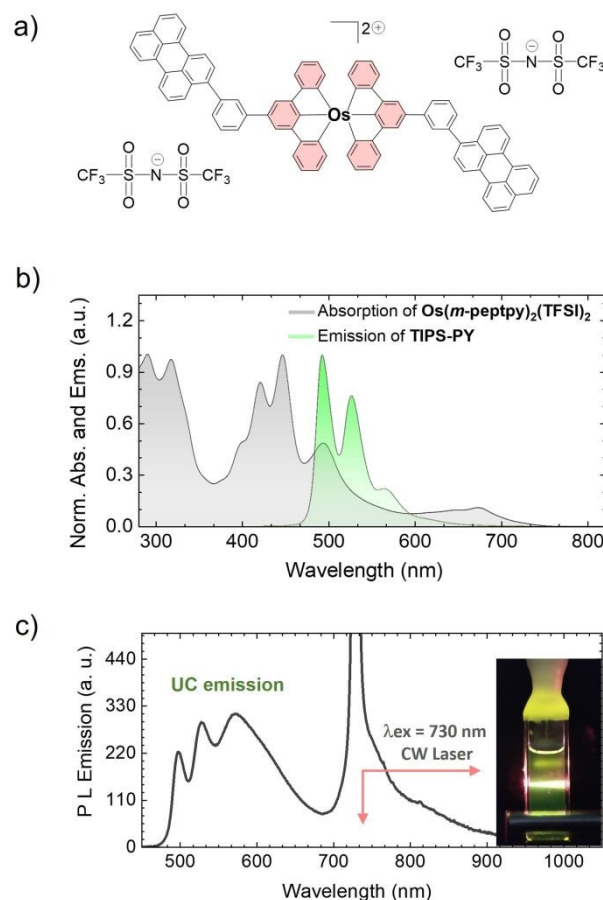


Fig. 6. a) Molecular structure of **Os(m-peptpy)₂(TFSI)₂**. b) Absorption spectrum of **Os(m-peptpy)₂(TFSI)₂** and fluorescence emission spectrum of **TIPS-PY** (1mM) in the presence of **Os(m-peptpy)₂(TFSI)₂** (0.01mM) in DMF ($\lambda_{ex} = 420 \text{ nm}$). c) Upconversion emission spectrum of **TIPS-PY:Os(m-peptpy)₂(TFSI)₂** (1mM:0.01mM) system ($\lambda_{ex} = 730 \text{ nm}$ CW laser). d) Digital image of the yellow-green UC emission upon 730 nm CW laser excitation.

Conclusions

We synthesized a new green-emitting annihilator, **TIPS-PY** which exhibits the highest absolute TTA-UC quantum yield of 13.7% (50% theoretical maximum) for red-to-green (640 nm to 489 nm) TTA-UC upon combining with **PdTPBP** as a sensitizer. Such a high UC quantum yield is enabled by the combined effects of; 1) a high $\phi_{FL} = 95\%$ of **TIPS-PY**, 2) $\phi_{TET} \sim 100\%$ due to exothermic triplet energy transfer from **PdTPBP** to **TIPS-PY**, 3) miniscule secondary inner filter effects due to minimum spectral overlap of **PdTPBP** absorption and **TIPS-PY** emission, and 4) a high f value of $39.2\% \pm 2.4\%$ of **TIPS-PY**, which generated a high singlet population after triplet-coupling. Further investigations of the f factor from the TheoDORE program revealed a singlet-like character of the triplet pair state of **TIPS-PY** induced by the higher charge transfer character of the S_0S_1 excitations of **TIPS-PY** compared to **PY**. This may increase the coupling of the triplet-pair state with the excited singlet state of **TIPS-PY** to generate high singlet



population after triplet-triplet annihilation according to the Merrifield model. Interestingly, this behaviour was also observed for other TIPS-functionalized annihilators like **TIPS-BP**, having a similar transition dipole axis to that of **PY**, which was not previously explored. The obtained ϕ_{UC} and f values for **TIPS-PY** are among the highest for annihilators in the green-to-red spectral range and outperform well-known annihilators such as **PY**, **BPEA**, **mB-PY**, **rubrene** or **DPPs**.

Author contributions

P.B., L.N. and K.M.P. conceptualized the idea of this work. M.M. synthesized the TIPS-Perylene. P. B. and M. M. carried out primary photophysical characterization. L.N., M. D., E.R, G. K., P. B. and K. K. carried out UC and time resolved measurements. C. A. and M. S. carried out computational calculations. Y. S., N. Y. and N. K. synthesized Os-complex. P.B., L.N. and K.M.P. wrote the first draft of the manuscript. All authors contributed to the analysis of results in their respective parts and editing of the manuscript.

Conflicts of interest

There are no conflicts to declare.

Data availability

The original datasets generated and analyzed during the current study are available from the corresponding author on reasonable request. This data will have open access at *Zenodo* after publication of the manuscript.

Acknowledgements

L. N. acknowledges the Erasmus+ Traineeship Program, P. B. and M. M. acknowledge financial support from the La-Caixa junior research leadership-post doctoral program (ID: 100010434, fellowship code: LCF/BQ/P122/11910023) the State Investigation Agency, through the Severo Ochoa Programme for Centres of Excellence in R&D (CEX2023-001263-S) and project PID2021-123873NB-I00 for financial support. L. N. and A. B. P. acknowledge the start-up funds provided by the University of California San Diego and the use of facilities and instrumentation supported by NSF through the UC San Diego Materials Research Science and Engineering Center (UCSD MRSEC), grant # DMR-2011924. K. M. P. acknowledges funding from the European Research Council (No. 101002131), the Swedish Energy Agency, the Göran Gustafsson Foundation, the Swedish Research Council, Swedish Research Council Formas, the European Research Council (ERC) under grant agreement CoG, PHOTHEM - 101002131, the Catalan Institute of Advanced Studies (ICREA), and the European Union's Horizon 2020 Framework Programme under grant agreement no. 951801. M. D., G. K., K. K., acknowledge the "Universities' Excellence Initiative" programme by the Ministry of Education, Science and Sports of the Republic of Lithuania under the agreement with the Research Council of Lithuania (project No. S-A-UEI-23-6). M.S. is grateful for financial support from the Agencia Española de Investigación ((MCIN/AEI/10.13039/501100011033) for projects RED2022-134939-T, PID2020-113711GB-I00 and PID2023-147424NB-I00 funded by Generalitat de Catalunya for Project

2021SGR623 and ICREA Academia 2025 prize. N.Y. acknowledges the support by JSPS KAKENHI (JP23H00304). N.K. acknowledges the support by JSPS KAKENHI (JP20H05676).

Notes

Supporting Information-1

Synthesis, NMR, MALDI-TOF, and X-Ray Diffraction analysis of **TIPS-PY** together with photophysical and upconversion measurements and DFT calculations. The authors have cited additional references within the Supporting Information.^{66–86}

Supporting Information-2

Cartesian coordinates of the species studied for computational calculations

References

- P. Bharmoria, H. Bildirir, K. Moth-Poulsen, *Chem. Soc. Rev.* **2020**, *49*, 6529–6554.
- F. Auzel, *Chem. Rev.* **2004**, *104*, 139–174.
- M. Wu, D. N. Congreve, M. W. B. Wilson, J. Jean, N. Geva, M. Welborn, T. Van Voorhis, V. Bulovic, M. G. Bawendi, M. A. Baldo, *Nat. Photonics* **2016**, *10*, 31–34.
- T. Schloemer, P. Narayanan, Q. Zhou, E. Belliveau, M. Seitz, D. N. Congreve, *ACS Nano* **2023**, *17*, 4, 3259–3288.
- L. Naimovičius, P. Bharmoria, K. Moth-Poulsen, *Mater. Chem. Front.* **2023**, *7*, 2297–2315.
- B. D. Ravetz, A. B. Pun, E. M. Churchill, D. N. Congreve, T. Rovis, L. M. Campos, *Nature* **2019**, *565*, 343–346.
- Q. Liu, M. Xu, T. Yang, B. Tian, X. Zhang, F. Li, *ACS Appl. Mater. Interfaces* **2018**, *10*, 9883–9888.
- Y. Sasaki, M. Oshikawa, P. Bharmoria, H. Kouno, A. Hayashi-Takagi, M. Sato, I. Ajioka, N. Yanai, N. Kimizuka, *Angew. Chem. Int. Ed.* **2019**, *58*, 17827–17833.
- S. N. Sanders, T. H. Schloemer, M. K. Gangishetty, D. Anderson, M. Seitz, A. O. Gallegos, R. C. Stokes, D. N. Congreve, *Nature* **2022**, *604*, 474–478.
- D. K. Limberg, J. H. Kang, R. C. Hayward, *J. Am. Chem. Soc.* **2022**, *144*, 5226–5232.
- A. J. Carrod, V. Gray, K. Börjesson, *Energy Environ. Sci.* **2022**, *15*, 4982–5016.
- R. E. Merrifield, *J. Chem. Phys.* **1968**, *48*, 4318–4319.
- R. E. Merrifield, *Pure Appl. Chem.* **1971**, *27*, 481–498.
- A. Olesund, J. Johnsson, F. Edhborg, S. Ghasemi, K. Moth-Poulsen, B. Albinsson, *J. Am. Chem. Soc.* **2022**, *144*, 3706–3716.
- A. Monguzzi, R. Tubino, S. Hoseinkhani, M. Campione, F. Meinardi, *Phys. Chem. Chem. Phys.* **2012**, *14*, 4322–4332.
- D. Casanova, Theoretical modeling of singlet fission. *Chem. Rev.* **2018**, *118*, 7164–7207.
- A. J. Carrod, V. Gray, K. Börjesson, *Energy Environ. Sci.*, **2022**, *15*, 4982–5016.
- D.-G. Ha, R. Wan, C. A. Kim, T.-A. Lin, L. Yang, T. Van Voorhis, M. A. Baldo, M. Dincă, *Nat. Mater.* **2022**, *21*, 1275–1281.
- M. B. Smith, J. Michl, *Chem. Rev.* **2010**, *110*, 6891–6936.
- N. Harada, Y. Sasaki, M. Hosoyamada, N. Kimizuka, N. Yanai, *Angew. Chem. Int. Ed.* **2021**, *60*, 142–147.
- V. Gray, A. Dreos, P. Erhart, B. Albinsson, K. Moth-poulsen, M. Abrahamsson, *Phys. Chem. Chem. Phys.* **2017**, *19*, 10931–10939.
- A. Olesund, V. Gray, J. Mårtensson, B. Albinsson, *J. Am. Chem. Soc.* **2021**, *143*, 5745–5754.
- D. Beljonne, A. Rao, *ACS Mater. Lett.* **2019**, *1*, 660–664.



- 24 A. J. Carrod, A. Cravcenco, C. Ye, K. Börjesson, *J. Mater. Chem. C* **2022**, *10*, 4923–4928.
- 25 C. Ye, V. Gray, K. Kushwaha, S. Kumar Singh, P. Erhart, K. Börjesson, *Phys. Chem. Chem. Phys.* **2020**, *22*, 1715–1720.
- 26 E. Radiunas, S. Raišys, S. Juršėnas, A. Jozeliūnaitė, T. Javorskis, U. Šinkevičiūtė, E. Orentas, K. Kazlauskas, *J. Mater. Chem. C* **2020**, *8*, 5525–5534.
- 27 E. Radiunas, L. Naimovičius, S. Raišys, A. Jozeliūnaitė, E. Orentas, K. Kazlauskas, *J. Mater. Chem. C* **2022**, *10*, 6314–6322.
- 28 E. Radiunas, M. Dapkevičius, L. Naimovičius, P. Baronas, S. Raišys, S. Juršėnas, A. Jozeliūnaitė, T. Javorskis, U. Šinkevičiūtė, E. Orentas, K. Kazlauskas, *J. Mater. Chem. C* **2021**, *9*, 4359–4366.
- 29 D. G. Bossanyi, Y. Sasaki, S. Wang, D. Chekulaev, N. Kimizuka, N. Yanai, J. Clark, *JACS Au* **2021**, *1*, 2188–2201.
- 30 W. S. Y. Cheng, B. Fackel, T. Khoury, R. G. C. R. Clady, M. J. Y. Tayebjee, N. J. Ekins-Daukes, M. J. Crossley, *J. Phys. Chem. Lett.* **2010**, *1*, 1795–1799.
- 31 A. B. Pun, L. M. Campos, D. N. Congreve, *J. Am. Chem. Soc.* **2019**, *141*, 3777–3781.
- 32 L. Naimovičius, E. Radiunas, B. Chatinowska, A. Jozeliūnaitė, E. Orentas, K. Kazlauskas, *J. Mater. Chem. C* **2023**, *11*, 698–704.
- 33 G. Alachouzos, A. M. Schulte, A. Mondal, W. Szymanski, B. L. Feringa, *Angew. Chem. Int. Ed.* **2022**, *61*, e202201308.
- 34 A. K. Singh, S. Banerjee, A. V. Nair, S. Ray, M. Ojha, A. Mondal, N. D. P. Singh, *ACS Appl. Bio. Mater.* **2022**, *5*, 1202–1209.
- 35 K. R. Konrad, S. Gao, M. D. Zurbriggen, G. Nagel, *Annu. Rev. Plant Biol.* **2023**, *74*, 313–339.
- 36 K.-N. Chen, B.-G. Ma, *ACS Synth. Biol.* **2023**, *12*, 1708–1715.
- 37 S. H. C. Askes, M. Klotz, G. Bruylants, J. T. M. Kennis, S. Bonnet, *Phys. Chem. Chem. Phys.* **2015**, *17*, 27380–27390.
- 38 I. Terashima, T. Fujita, T. Inoue, W. S. Chow, R. Oguchi, *Plant Cell Physiol.* **2009**, *50*, 684–97.
- 39 F. Plasser, *J. Chem. Phys.* **2020**, *152*, 084108.
- 40 L. Zeng, L. Huang, W. Lin, L. H. Jiang, G. Han, *Nat. Commun.* **2023**, *14*, 1102.
- 41 M. Tracy, S. Singh, *Sony Corp* **2016**, WO2017197144A1.
- 42 L. Naimovičius, E. Radiunas, M. Dapkevičius, P. Bharmoria, K. Moth-Poulsen, K. Kazlauskas, *J. Mater. Chem. C* **2023**, *11*, 14826–14832.
- 43 A. J. Carrod, A. Cravcenco, C. Ye, K. Börjesson, *J. Mater. Chem. C* **2022**, *10*, 4923–4928.
- 44 J. E. Rogers, K. A. Nguyen, D. C. Hufnagle, D. G. McLean, W. Su, K. M. Gossett, A. R. Burke, S. A. Vinogradov, R. Pachter, P. A. Fleitz, *J. Phys. Chem. A* **2003**, *107*, 11331–11339.
- 45 R. Englman and J. Jortner, *Mol. Phys.* **1970**, *18*, 145.
- 46 W. Siebrand, *J. Chem. Phys.* **1967**, *47*, 2411–2422.
- 47 S. J. Jang, *J. Chem. Phys.* **2021**, *155*, 164106-1–164106-9.
- 48 R. C. Johnson, R. E. Merrifield, *Phys. Rev. B* **1970**, *1*, 896–902.
- 49 M. Gudem, M. Kowalewski, *Chem. Eur. J.* **2022**, *28*, e202200781.
- 50 K. C. Krishnapriya, P. Roy, B. Puttaraju, U. Salzner, A. J. Musser, M. Jain, J. Dasgupta, S. Patil, *Nat. Commun.*, **2019**, *10*, 33.
- 51 K. Miyata, F. S. Conrad-Burton, F. L. Geyer, X.-Y. Zhu, *Chem. Rev.* **2019**, *119*, 4261–4292.
- 52 H.-S. Im, E. R. Bernstein, *J. Chem. Phys.* **1988**, *88*, 12.
- 53 P. Yan, A. Chowdhury, M. W. Holman, D. M. Adams, *J. Phys. Chem. B* **2005**, *109*, 724–730.
- 54 J. A. Moghtader, M. Uji, T. J. B. Zähringer, M. Schmitz, L. M. Carrella, A. Heckel, E. Rentschler, N. Yanai, C. Kerzig, *ChemRxiv* **2025**, DOI: 10.26434/chemrxiv-2025-9prp7.
- 55 A. Olesund, J. Johnsson, F. Edhborg, S. Ghasemi, K. Moth-Poulsen, B. Albinsson, *J. Am. Chem. Soc.* **2022**, *144*, 3706–3716.
- 56 C. Brand, W. L. Meerts, M. Schmitt, *J. Phys. Chem. A* **2011**, *115*, 9612–9619.
- 57 P. Kimbert and F. Plasser, *J. Chem. Theory Comput.* **2023**, *19*, 2340–2352.
 View Article Online
DOI: 10.1039/D5SC05248C
- 58 [56] Y. Murakami, K. Kamada, *Phys. Chem. Chem. Phys.* **2021**, *23*, 18268–18282.
- 59 Y. Zhou, F. N. Castellano, T. W. Schmidt, K. Hanson, *ACS Energy Letters*, **2020**, *5*, 2322–2326.
- 60 P. Baronas, J. Lekavičius, M. Majdecki, J. L. Elholm, K. Kazlauskas, P. Gawel, K. Moth-Poulsen, *ACS Cent. Sci.* **2025**, *11*, 413–421.
- 61 E. Radiunas, L. Naimovičius, P. Baronas, A. Jozeliūnaitė, E. Orentas, K. Kazlauskas, *Adv. Opt. Mater.* **2025**, *13*, 2403032.
- 62 L. Naimovičius, S. K. Zhang, A. B. Pun, *J. Mater. Chem. C* **2024**, *12*, 18374–18380.
- 63 F. Edhborg, A. Olesund, B. Albinsson, *Photochem. & Photobiol. Sci.* **2022**, *21*, 1143–1158.
- 64 A. J. Carrod, A. Cravcenco, C. Ye, K. Börjesson, *J. Mater. Chem. C*, **2022**, *10*, 4923–4928.
- 65 Y. Sasaki, N. Yanai, N. Kimizuka, *Inorg. Chem.* **2022**, *61*, 5982–5990.
- 66 M. Tracy, S. Singh, *Sony Corp*, **2016**, WO2017197144A1.
- 67 J.-H. Kim, C. E. Song, I.-N. Kang, W. S. Shind, D.-H. Hwang, *Chem. Commun.* **2013**, *49*, 3248–3250.
- 68 G. M. Sheldrick, *Acta Crystallogr. Sect. A Found. Crystallogr.* **2015**, *71*, 3–8.
- 69 G. M. Sheldrick, *Acta Crystallogr. Sect. C Struct. Chem.* **2015**, *71*, 3–8.
- 70 O. V. Dolomanov, L. J. Bourhis, R. J. Gildea, J. A. K. Howard, H. Puschmann, *J. Appl. Crystallogr.* **2009**, *42*, 339–341.
- 71 C. Adamo, V. Barone, *J. Chem. Phys.* **1999**, *110*, 6158–6170.
- 72 S. Grimme, J. Antony, S. Ehrlich, H. Krieg, *J. Chem. Phys.* **2010**, *132*, 154104.
- 73 E. R. Johnson, A. D. Becke, *J. Chem. Phys.* **2005**, *123*, 024101.
- 74 A. D. Becke, E. R. Johnson, *J. Chem. Phys.* **2005**, *123*, 154101.
- 75 R. Krishnan, J. S. Binkley, R. Seeger, J. A. Pople, *J. Chem. Phys.* **1980**, *72*, 650–654.
- 76 M. J. Frisch, G. W. Trucks, H. B. Schlegel, G. E. Scuseria, M. A. Robb, J. R. Cheeseman, G. Scalmani, V. Barone, G. A. Petersson, H. Nakatsuji, X. Li, M. Caricato, A. V. Marenich, J. Bloino, B. G. Janesko, R. Gomperts, B. Mennucci, H. P. Hratchian, J. V. Ortiz, A. F. Izmaylov, J. L. Sonnenberg, D. Williams-Young, F. Ding, F. Lipparini, F. Egidi, J. Goings, B. Peng, A. Petrone, T. Henderson, D. Ranasinghe, V. G. Zakrzewski, J. Gao, N. Rega, G. Zheng, W. Liang, M. Hada, M. Ehara, K. Toyota, R. Fukuda, J. Hasegawa, M. Ishida, T. Nakajima, Y. Honda, O. Kitao, H. Nakai, T. Vreven, K. Throssell, J. A. Montgomery Jr., J. E. Peralta, F. Ogliaro, M. J. Bearpark, J. J. Heyd, E. N. Brothers, K. N. Kudin, V. N. Staroverov, T. A. Keith, R. Kobayashi, J. Normand, K. Raghavachari, A. P. Rendell, J. C. Burant, S. S. Iyengar, J. Tomasi, M. Cossi, J. M. Millam, M. Klene, C. Adamo, R. Cammi, J. W. Ochterski, R. L. Martin, K. Morokuma, O. Farkas, J. B. Foresman, D. J. Fox, *Gaussian 16 Rev. C.01*, Wallingford, CT, **2016**.
- 77 C. Lee, W. Yang, R. G. Parr, *Phys. Rev. B* **1988**, *37*, 785–789.
- 78 A. D. Becke, *J. Chem. Phys.* **1993**, *98*, 5648–5652.
- 79 F. Plasser, *J. Chem. Phys.* **2020**, *152*, 084108.
- 80 M. R. Padhye, S. P. McGlynn, M. Kasha, *J. Chem. Phys.* **1956**, *24*, 588–594.
- 81 J. S. Brinen, J. G. Koren, *Chem. Phys. Lett.* **1968**, *2*, 671–672.
- 82 J. K. H. Pun, J. K. Gallaher, L. Frazer, S. K. K. Prasad, C. B. Dover, R. W. MacQueen and T. W. Schmidt, *J. Photonics Energy*, **2018**, *8*, 1.
- 83 R. H. Clarke, R. M. Hochstrasser, *J. Mol. Spectrosc.* **1969**, *32*, 309–319.
- 84 E. M. Gholizadeh, S. K. K. Prasad, Z. L. Teh, T. Ishwara, S. Norman, A. J. Petty, J. H. Cole, S. Cheong, R. D. Tilley, J. E. Anthony, S. Huang, T. W. Schmidt, *Nat. Photonics* **2020**, *14*, 585–590.



ARTICLE

Journal Name

- 85 T. N. Singh-Rachford, F. N. Castellano, *J. Phys. Chem. A* **2008**, *112*, 3550–3556.
- 86 J. C. De Mello, H. F. Wittmann, R. H. Friend, *Adv. Mater.* **1997**, *230*–232.

View Article Online
DOI: 10.1039/D5SC05248C





Barcelona, July 15, 2025

To whom it may concern

In reference to the data related to the manuscript "Enhancing the Statistical Probability Factor in Triplet-Triplet Annihilation Photon Upconversion via TIPS Functionalization" by Lukas Naimovičius, Manvydas Dapkevičius, Edvinas Radiunas, Mila Miroshnichenko, Gediminas Kreiza, Carles Alcaide, Paulius Baronas, Nobuhiro Yanai, Nobuo Kimizuka, Andrew B. Pun, Miquel Solà, Pankaj Bharmoria, Karolis Kazlauskas, Kasper Moth-Poulsen.

The data supporting this article have been included as part of the Supplementary Information.

Sincerely,

Kasper Moth-Poulsen, on behalf of all authors.

ICREA Professor, FRSC

Elected member of the Royal Swedish Academy of Engineering Science
Associate Editor of J. Mater. Chem. C. & Materials AdvancesPolytechnic University of Catalunya (UPC),
Institut de Ciència de Materials de Barcelona (ICMAB-CSIC)
Chalmers University of Technology, Gothenburg, Swedenwww.moth-poulsen.com
@kmothpoulsen